Tropical Cyclones: Secondary Eyewall Formation

C-C Wu and Y-H Huang, National Taiwan University, Taipei, Taiwan

Synopsis

Secondary eyewall formation (SEF), a phenomenon often observed in intense tropical cyclones (TCs), is one of the key issues for TC research and forecasting as indicated by the widely documented findings related to the increase in storm size and short-term changes in TC intensity. This review article provides a comprehensive summary and discussions of current understandings of the plausible physical mechanisms for SEF in the literature. Provided with a favorable moist environment, a variety of internal dynamical processes for SEF have been proposed, such as the axisymmetrization process, energy accumulation through vortex Rossby wave activities, beta-skirt-induced energy cascade, unbalanced responses to boundary layer dynamics, and the balanced response to convective heating. The merits and caveats among different dynamical interpretations are discussed, while prominent unsolved SEF issues are also addressed to provide valuable guidance for future SEF research.

Background

Secondary eyewall formation (SEF) and the eyewall replacement cycle in tropical cyclones (TCs) have been widely documented by aircraft observations and high-resolution satellite imagery. Two concentric quasi-circular deep convective rings (inner and outer TC eyewalls) and a nearly cloud-free region (moat) located in between can be easily identified during the double-eyewall episode in TCs (Figure 1). For most such cases, the outer eyewall is established later, with characteristics similar to the inner eyewall. A local maximum swirling wind is often present in the outer eyewall, with the strong swirling wind region confined to the lower- or midtroposphere. Statistical analyses based on a 10-year data set (1997–2006) showed that on average 70% of the Atlantic, 50% of the eastern Pacific, 40% of the Southern Hemisphere, and 80% of the western Pacific intense storms (maximum wind >120 kts) underwent at least one eyewall replacement cycle during their lifetime. Consistent statistical results were also obtained in recent studies, showing that SEF is a relatively common phenomenon in intense TCs. Because SEF, along with the subsequent eyewall replacement cycle, is often associated with temporary weakening of storms and concomitant increase in the extent of damaging gale-force winds, it remains as an important forecast priority for populated coastal communities and seagoing vessels over the open ocean.

Numerical simulations have been extensively applied to investigate SEF in many previous studies. Based on physical

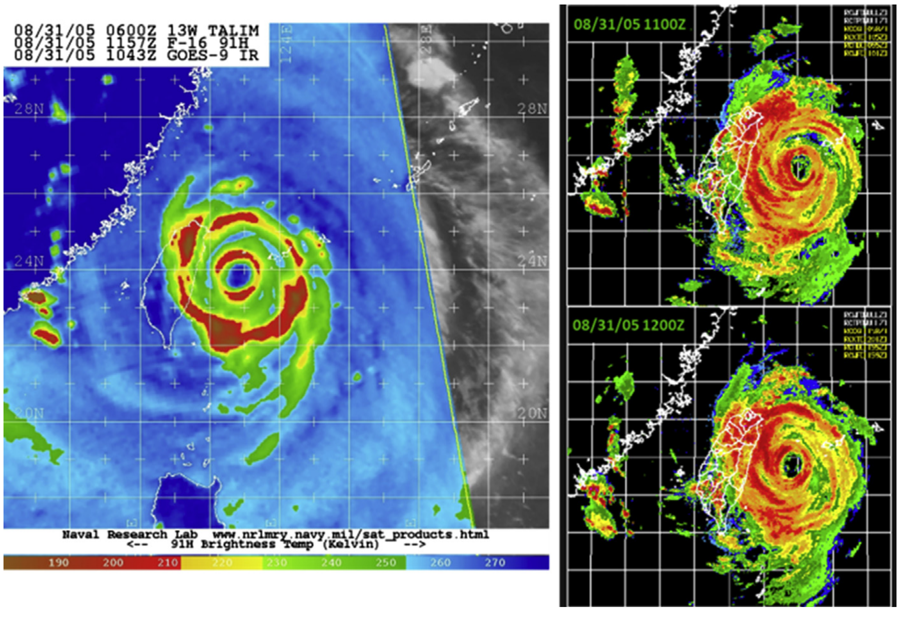

Figure 1 Concentric eyewalls in Typhoon Talim (2005) near Taiwan. The figure on the left is the image retrieved from the Special Sensor Microwave Imager/Sounder sensor on the Defense Meteorological Satellite Program satellite at 1157 UTC 31 August 2005, available at the NRL (Naval Research Laboratory) Tropical Cyclone Page (www.nrlmry.navy.mil). The panel on the right contains radar images of composite reflectivity (dBz) at 1100 and 1200 UTC 31 August 2005, provided by the Central Weather Bureau (CWB) of Taiwan.

analyses and sensitivity experiments among numerical studies, a number of factors and mechanisms have been suggested as contributors to SEF. Section Environmental Conditions introduces the possible roles of various environmental conditions in SEF. As for the internal mechanisms responsible for SEF, there are a number of hypotheses proposed in the literature. Recent studies have found that the physical constraints applied to some hypotheses are not able to fully capture the physical processes involved in the life cycle of a real SEF event. Numerical simulations with more sophisticated physical processes, such as diabatic heating and boundary layer processes, suggested that some of the proposed hypotheses could not adequately address the key internal mechanisms of SEF in a real TC. The details of the aforementioned hypotheses are introduced and discussed in Section Internal Mechanisms of SEF. Finally, Section Vortex Rossby Waves contains the concluding remarks upon the current understanding of SEF and proposes key issues to be further investigated.

Environmental Conditions

Environmental moisture is one of the major factors affecting TC intensity and structure. Numerical models with different designs have been adopted to study the impact of ambient relative humidity on SEF. In the axisymmetric model framework, high relative humidity is critical to SEF only if the hydrostatic assumption is applied. In contrast, full-physics model simulations showed that high environmental relative humidity is crucial to the formation of an outer eyewall in a TC. A plausible explanation is that high ambient humidity can provide more moisture and thus can enhance latent heat release in the vortex's outer core region, which likely provides a favorable environment for the expansion of storm size, the formation/intensification of rainbands, and even SEF. Another elucidation for the environmental influence on SEF is the sustained eddy angular momentum fluxes caused by interactions between a mature TC and its environment. If this TC–environment interaction is sufficiently influential in strength and space that gives rise to the Wind-Induced Air-Sea Heat Exchange (WISHE) process, a secondary eyewall likely establishes outside the primary eyewall.

Internal Mechanisms of SEF

Five internal mechanisms that have been frequently discussed in existing SEF studies are introduced and discussed in the subsections below, which are titled vortex Rossby waves (VRWs), axisymmetrization process, beta-skirt axisymmetrization (BSA) formation hypothesis, unbalanced boundary layer dynamics near the top of TC boundary layer, and balanced response to diabatic heating in a region of enhanced inertial stability.

Vortex Rossby Waves

Based on radar and satellite images, it has been found that disturbances with similar characteristics to Rossby waves are often associated with rainbands in TCs. VRWs are thus coined for these eddy activities in TCs. Similar to Rossby waves in a planetary system, the dispersion relation for VRWs is closely related to the vorticity gradient of TCs. In a dry and barotropic framework, Montgomery and Kallenbach obtained an analytic solution of the stagnation radius for VRWs that propagate radially outward from the eyewall. It has then been proposed that the accumulation of energy near that stagnation radius can have impacts on the outer rainband structure and perhaps on the formation of secondary wind maximum. Houze and colleagues found that the model failed to simulate the eyewall replacement cycle of Hurricane Rita (2005), when the model resolution was reduced from 1.67 to 5 km. Meanwhile, they noticed that during Rita's eyewall replacement cycle, the small-scale features captured by the radar in the inner core region may be related to the VRWs' dynamics. The importance of high model resolution and the value of targeting small-scale structures in TCs are thus suggested for a better understanding of SEF and the subsequent eyewall replacement cycle. In contrast to consensus on the role of VRWs in TC rainbands, some recent studies argued the role of VRWs in SEF by using the model results with more sophisticated physical processes. Judt and Chen indicated that the near-zero potential vorticity (PV) gradient, subsidence, and straining effect which are already present prior to SEF are not conducive for VRWs' outward propagation, and thus provided reasonable doubt against the essential role of VRWs in SEF. Noting the ambiguous role of the eddy fluxes associated with VRWs in speeding up the tangential wind in the SEF region, Corbosiero and colleagues inferred that the outward propagation of the convectively coupled VRWs from the inner eyewall may act to redistribute PV and dump out moisture at the stagnation radius. It was thus suggested that VRWs make the active convection more prominent, but not to the extent that would directly cause SEF.

Axisymmetrization Process

Drawing from studies of vortex dynamics, the axisymmetrization process has been used to interpret the formation of vorticity ring outside the parent vortex in a two-dimensional barotropic model. Kuo and colleagues suggested that the primary vortex can axisymmetrize weak vorticity patches into a vorticity ring, provided that the primary vortex is strong enough and the two vortices are sufficiently close to each other. Nevertheless, recent studies noted that PV patches outside the eyewall can be of comparable magnitude to that in the eyewall region and have dipole structures in the real TC environment as simulated with more realistic physical processes (such as the moist convection). In particular, Moon and colleagues demonstrated that the interaction between the TC core vortex and the convection-induced small vorticity dipoles of considerable strength in two-dimensional flows does not lead to the formation of a coherent concentric vorticity ring. Thus the axisymmetrization process under a simplified two-dimensional incompressible flow appears insufficient for describing SEF in the real atmosphere. The critical role of the three-dimensional moist process in the maintenance of a vorticity ring has also been shown in recent studies.

Beta-Skirt Axisymmetrization Formation Hypothesis

Terwey and Montgomery presented a new moist-based BSA formation hypothesis as an intrinsic SEF mechanism. This hypothesis requires a region with sufficiently long filamentation time and moist convective potential, a sufficient low-level radial PV gradient (i.e., a beta skirt) associated with the primary swirling flow and the follow-up WISHE process. The long filamentation time and sufficient moist convective potential set the scene for a convectively favorable environment. The beta-skirt structure and WISHE process provide a dynamical pathway to SEF. Applying the two-dimensional turbulence theory to the problem of SEF in a rotating TC environment, the theme of the BSA hypothesis is that the upscale energy cascade tends to occur on the beta skirt. Following this pathway, eddy kinetic energy associated with the sporadic convective cells outside the primary eyewall may be injected into the tangential direction and enhance local low-level jets (axisymmetrized into the mean tangential flow) on the skirt of the vortex's PV profile. Once the low-level jet strengthens substantially, it could further intensify by coupling with the boundary layer through a wind-induced moisture feedback process such as WISHE and may ultimately lead to SEF. The timescale of this energy cascade process and the width of the corresponding jet can be evaluated by the values of its PV gradient. Though simulated results in relevant studies showed consistency between the evaluated and simulated jet width, direct supporting evidence for the described energy upscale process needs to be further investigated.

Unbalanced Boundary Layer Dynamics near the Top of TC Boundary Layer

A deeper understanding of the underlying dynamics of SEF has been proposed in two recent companion studies, based on the two mechanisms for the spin-up of mean tangential winds in single-eyewall TCs. Both mechanisms are associated with the radial advection of absolute angular momentum ($M = fr^2/2 + rv$). The first mechanism is for the spin-up above the boundary layer where M is materially conserved. The convergence of M is enhanced by the negative radial gradient of a diabatic heating rate associated with convective structures in a TC. This mechanism has been addressed in many extant studies. It explains why the vortex expands in size in terms of axisymmetric balanced dynamics, wherein the vortex is well approximated by gradient wind and hydrostatic balance. The second mechanism is related to the spin-up process within the boundary layer and is considered important in the inner core region of the storm. Although M is not materially conserved here, tangential winds can still be enhanced if the boundary layer inflow is sufficiently large to bring the air parcels to the small radii with minimal loss of M to friction. The boundary layer flow is coupled to the interior flow via the radial pressure gradient at the top of the boundary layer, but the spin-up of a vortex is ultimately tied to the dynamics of the boundary layer where inflow is prevailing and the swirling wind is not in gradient wind balance over a substantial radial span.

By assimilating T-PARC (THORPEX Pacific Asian Regional Campaign) data (particularly aircraft reconnaissance and surveillance observations) into the Weather Research and Forecasting (WRF) model based on ensemble Kalman filter data assimilation, Wu and colleagues constructed a model/observation-consistent and high-spatial/temporal resolution data set for Typhoon Sinlaku (2008) in the first part of the two companion works. The key features related to the horizontal broadening of low-level troposphere swirling flow and intensification of boundary layer inflow over the outer region are identified before SEF (Figure 2). These two important features are consistent with the two mechanisms highlighted for the spin-up of single-eyewall TCs and set the scene for a progressive boundary layer control pathway to SEF.

As the second part of the two companion papers, Huang and colleagues addressed the association between increases in storm size and SEF from the axisymmetric aspect. The findings point to collective structural changes in the outer core region of a mature TC, which ultimately culminates in the formation of a secondary eyewall. The sequence begins with a broadening of the low-level tangential wind field associated with the intensification of the eyewall that can be demonstrated by the balanced response above the boundary layer (the first mechanism mentioned above). Due to the presence of surface friction, boundary layer inflow increases underneath the broadened swirling wind, and becomes large enough to enhance the swirling circulation within the boundary layer (the second spin-up mechanism). This rapid increase in tangential winds near the top of the boundary layer breaks the gradient wind balance, leading to the local development of supergradient winds, which decelerate the inflow air parcels and impede them from moving inward (Figure 3). This process leads to the transition outside the primary eyewall from sporadic and/or weak convergence in the lower troposphere to a well-defined convergence zone concentrated within and just above the boundary layer. The progressive increase of supergradient forces thus continuously provides a mechanical mean for high enthalpy air to erupt from the boundary layer. Given the dynamically and thermodynamically favorable environment for convective activities, the progressive response of the unbalanced boundary layer flow to an expanding swirling wind field and the positive feedback loop in between are demonstrated to be an important mechanism for concentrating and sustaining deep convection in a narrow supergradient-wind zone collocated with the SEF region. The pathway to SEF can be summarized in a schematic diagram (Figure 4), elucidating the chain of TC structure changes and associated physical processes and feedbacks.

The SEF paradigm advanced in these two companion works is attractive on physical grounds because of its simplicity and consistency with the three-dimensional numerical simulations presented. While understanding the importance of the balanced response (cf Balanced Response to Diabatic Heating in a Region of Enhanced Inertial Stability subsection), this paradigm peculiarly highlights the critical role of unbalanced dynamics in SEF. Two recently published studies also investigated the impact of boundary layer dynamics on SEF from different perspectives. Concerning the asymmetry associated with rainbands that prevail prior to SEF, Qiu and Tan reexamined this SEF paradigm in an asymmetric framework. The sequence of structure changes

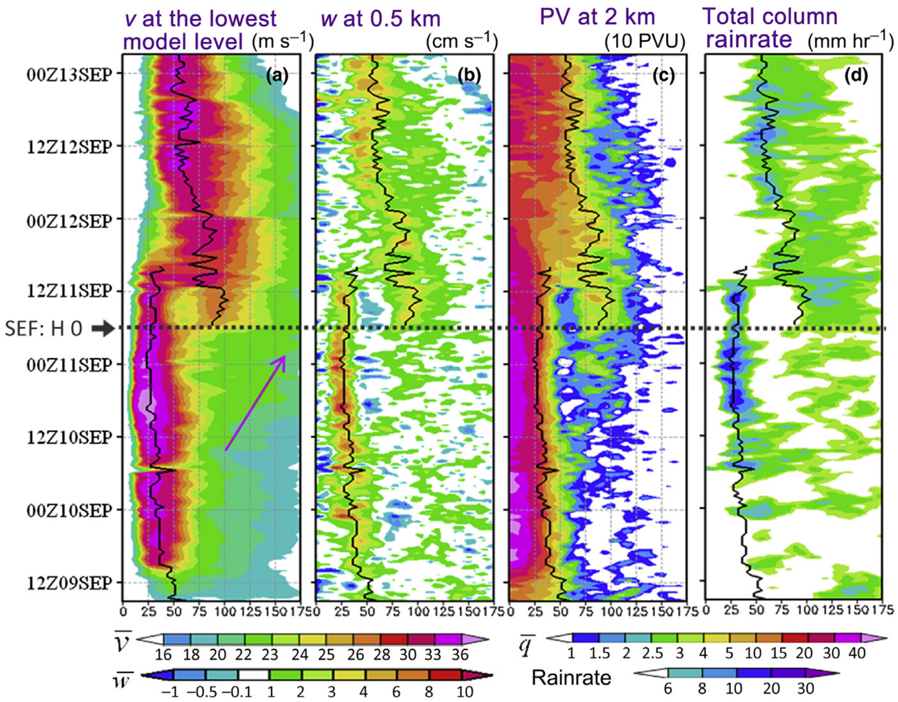

Figure 2 Time–radius diagrams of the azimuthally mean indicating (a) tangential wind (m s^{-1}) at the lowest model level, (b) vertical velocity (m s^{-1}) at 0.5 km height, (c) potential vorticity (10 (potential vorticity unit) PVU) at 2 km height, and (d) total column rainrate (mm h^{-1}) for the ensemble mean (average of 28 ensemble members). SEF time is indicated by a dotted line and an arrow on the *y* axis. The black solid lines are the radii of the local maxima in the surface tangential wind. Taken from Wu, C.-C., Huang, Y.-H., Lien, G.-Y., 2012. Concentric eyewall formation in Typhoon Sinlaku (2008). Part I: Assimilation of T-PARC data based on the ensemble Kalman filter (EnKF). Monthly Weather Review 140, 506–527.

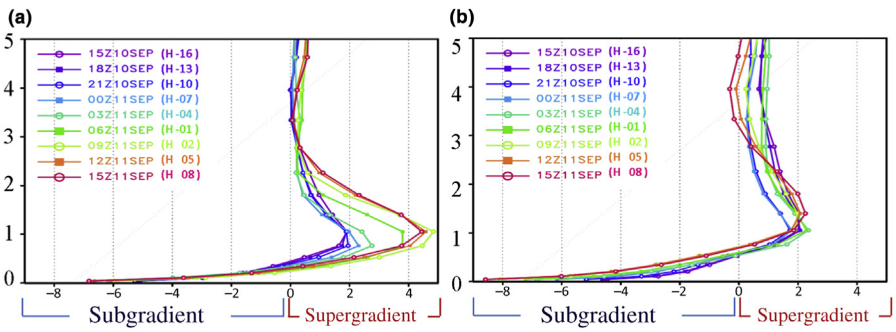

Figure 3 Azimuthally, area- and temporally averaged values over ($t-3$ h, $t+3$ h) for the agradient wind (unit: m s^{-1}). Analyses from 1500 UTC 10 Sep to 1500 UTC 11 Sep are displayed with a 3-h interval. The green line represents 1 h prior to SEF, while the light-green line represents 2 h after SEF. (a) SEF region ($r = 75 \sim 125$ km) and (b) outside SEF region ($r = 125 \sim 180$ km). Taken from Huang, Y.-H., Montgomery, M.T., Wu, C.-C., 2012. Concentric eyewall formation in Typhoon Sinlaku (2008). Part II: Axisymmetric dynamical processes. Journal of Atmospheric Sciences 69, 662–674.

within and just above the boundary layer preceding SEF and the corresponding dynamical pathway to SEF found in their simulation showed supporting results for the presented paradigm. Meanwhile, Wang and colleagues investigated the depth-integrated boundary layer flow, and demonstrated results that generally agree with the SEF pathway proposed in this paradigm.

The presented progressive boundary layer control on SEF also implies that the boundary layer scheme and its coupling to the above atmosphere need to be adequately represented in numerical models to improve the understanding of SEF, as well as the accuracy of SEF forecasts, including the timing and preferred radial intervals.

Balanced Response to Diabatic Heating in a Region of Enhanced Inertial Stability

As discussed in the previous subsection, responses of transverse circulation to a heating/momentum source/sink framed in the thermal wind balance relationship known as Sawyer–Eliassen equation, has been applied to understand the evolution of the mean swirling circulation in idealized vortices in many extant

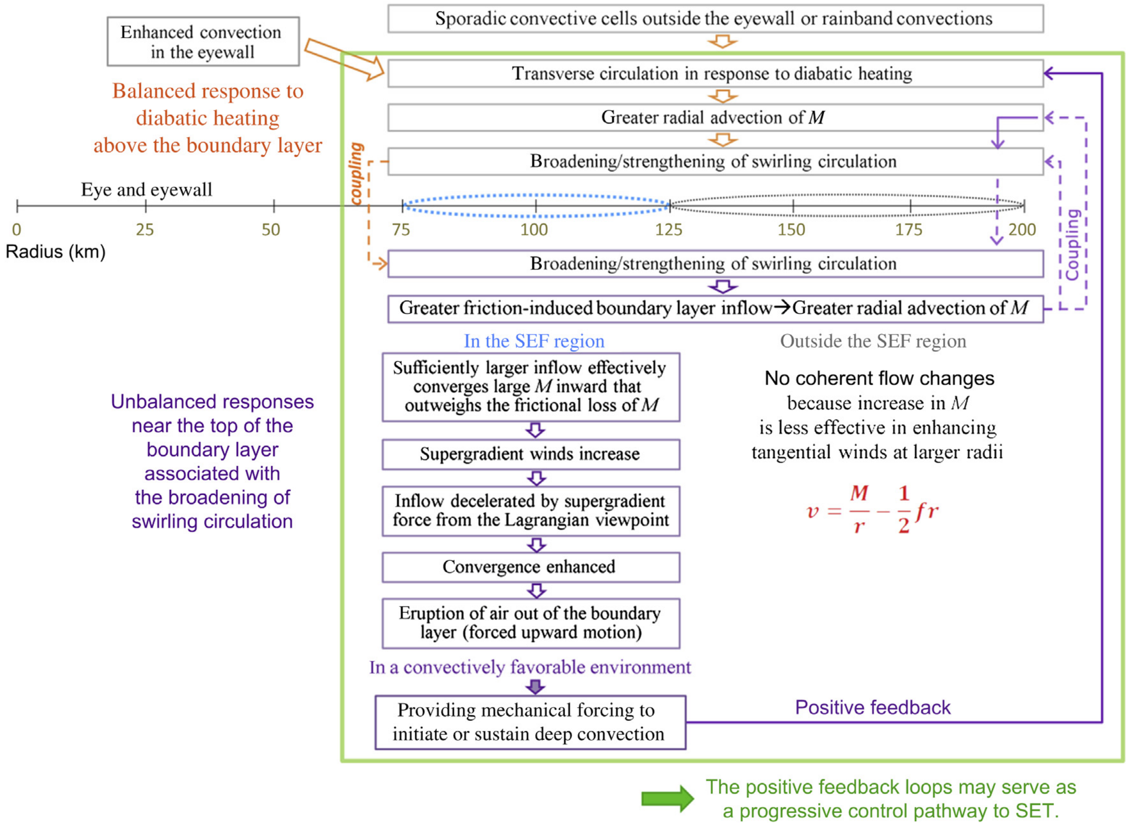

Figure 4 The schematic diagram describing the SEF paradigm introduced in Section Unbalanced Boundary Layer Dynamics near the Top of TC Boundary Layer. Orange arrows refer the balanced response to diabatic heating, which is constrained by the thermal wind relationship. Purple arrows indicate the unbalanced dynamics, characterized by the development of supergradient wind near the top of boundary layer and a chain of corresponding structure changes. Dashed lines stand for the coupling relationship between the boundary layer and the free atmosphere aloft. The positive feedback loop enclosed by the green box is shown as a progressive control pathway to SEF.

studies. Using an idealized, cloud-resolving WRF simulation, Rozoff and colleagues revisited the balanced dynamics for SEF from the axisymmetric aspects. An expansion of kinetic energy (or enhanced inertial stability) is found prior to the SEF in their WRF simulation, a feature consistent with the presence of beta-skirt structure and the expansion of tangential winds in previous studies. The impact of this enhanced kinetic energy and diabatic heating on SEF was further investigated using an axisymmetric linearized, nonhydrostatic model (a balanced vortex model quite similar to the Sawyer–Eliassen model). Given the axisymmetric tangential wind and temperature profiles from the WRF model output, this simple model depicts how the transverse circulation responds to diabatic heating and surface friction prescribed also from WRF. The diagnosed results share similarity with the mean vortex structure in the WRF simulation in a number of ways, and suggest that the sustained diabatic heating along with the broadening wind outside the primary eyewall contributes the most to the enhancement of tangential winds in the SEF region.

Concluding Remarks

This article revisits favorable conditions and mechanisms that have been suggested for SEF in the existing studies. Regarding the environmental control of SEF, model initial relative humidity has been identified critical for the increase of storm size and the subsequent SEF in recent studies using sophisticated numerical models. On the other hand, a variety of different approaches have been proposed as the internal mechanisms of SEF, including (1) axisymmetrization of prescribed/present outer vorticity patches, (2) the accumulation of eddy kinetic energy associated with VRWs near their stagnation radii, (3) the energy cascade process over the beta skirt of the TC vortex in a convectively favorable condition and subsequent positive feedback provided by WISHE (BSA hypothesis), (4) unbalanced response (i.e., the generation of supergradient wind, and its impact on the transverse circulation) to the expanding winds, and (5) balanced response of transverse circulation to diabatic heating over the area with enhanced inertial stability. Particularly noteworthy is that the broadening tangential wind (the beta-skirt structure and enhanced kinetic energy basically indicate a similar structure as well) furnishing the pathway to SEF is a vital process among different internal dynamical interpretations of SEF. Various conditions and mechanisms have been suggested for the establishment of such a skirted vortex structure, including higher environmental relative humidity or diabatic heating associated with outer rainbands, the initial vortex size/shape, concurrent storm intensity, convective heating in an intensifying storm, and radially outward propagating VRWs.

Although recent advances of the unbalanced and balanced dynamics in TCs with double eyewalls appear promising in interpreting SEF from the axisymmetric perspective, the quantitative impacts of the these aspects on SEF and their mutual feedback remain to be further investigated. While the symmetric dynamics has been shown to play a critical role in SEF, how the asymmetric components (e.g., spiral rainbands and sporadic convective cells in the vortex's outer core region) influence SEF also needs further studies to gain more comprehensive understanding. While the environmental conditions are relatively well understood and better presented in the observations and numerical models, discoveries are also being made on more uncertainties associated with the evolution of a TC vortex and the accompanied convective-scale features. More TC observations and further investigation on the internal vortex dynamics are thus required to better present the corresponding physical processes (e.g., microphysics, boundary layer dynamics, etc.) in numerical simulations of SEF, as well as the whole TC life cycle.

See also: **Mesoscale Meteorology:** Severe Storms. **Satellites and Satellite Remote Sensing:** Precipitation. **Tropical Cyclones and Hurricanes:** Hurricanes: Observation.

Further Reading

Corbosiero, K.L., Abarca, S., Montgomery, M.T., 2012. Vortex Rossby waves and secondary eyewall formation in a high-resolution simulation of Hurricane Katrina (2005). Proceedings of 30th Conference on Hurricanes and Tropical Meteorology. American Meteorological Society, Jacksonville, FL. 1A.6.
Hill, K.A., Lackmann, G.M., 2009. Influence of environmental humidity on tropical cyclone size. Monthly Weather Review 137, 3294–3315.
Houze Jr., R.A., Chen, S.S., Smull, B.F., Lee, W.-C., Bell, M.M., 2007. Hurricane intensity and eyewall replacement. Science 315, 1235–1239.
Huang, Y.-H., Montgomery, M.T., Wu, C.-C., 2012. Concentric eyewall formation in Typhoon Sinlaku (2008). Part II: Axisymmetric dynamical processes. Journal of Atmospheric Sciences 69, 662–674.
Judt, F., Chen, S.S., 2010. Convectively generated potential vorticity in rainbands and formation of the secondary eyewall in Hurricane Katrina of 2005. Journal of the Atmospheric Sciences 67, 3581–3599.
Kuo, H.-C., Schubert, W.H., Tsai, C.-L., Kuo, Y.-F., 2008. Vortex interaction and barotropic aspects of concentric eyewall formation. Monthly Weather Review 137, 5182–5198.
Montgomery, M.T., Kallenbach, R.J., 1997. A theory for vortex Rossby waves and its application to spiral bands and intensity changes in hurricanes. Quarterly Journal of the Royal Meteorological Society 123, 435–465.
Moon, Y., Nolan, D.S., Iskandarani, M., 2010. On the use of two-dimensional incompressible flow to study secondary eyewall formation in tropical cyclones. Journal of Atmospheric Sciences 67, 3765–3773.
Nong, S., Emanuel, K.A., 2003. A numerical study of the genesis of concentric eyewalls in hurricane. Quarterly Journal of the Royal Meteorological Society 129, 3323–3338.
Qiu, X., Tan, Z.-M., 2013. The roles of asymmetric inflow forcing induced by outer rainbands in tropical cyclone secondary eyewall formation. Journal of Atmospheric Sciences 70, 953–974.
Rozoff, C.M., Nolan, D.S., Kossin, J.P., Zhang, F., Fang, J., 2012. The roles of an expanding wind field and inertial stability in tropical cyclone secondary eyewall formation. Journal of Atmospheric Sciences 69, 2621–2643.
Terwey, W.D., Montgomery, M.T., 2008. Secondary eyewall formation in two idealized, full-physics modeled hurricanes. Journal of Geophysical Research 113, D12112.
Wang, Y., 2009. How do outer spiral rainbands affect tropical cyclone structure and intensity? Journal of Atmospheric Sciences 66, 1250–1273.
Wang, X., Ma, Y., Davidson, N.E., 2013. Secondary eyewall formation and eyewall replacement cycles in a simulated hurricane: effect of the net radial force in the hurricane boundary layer. Journal of Atmospheric Sciences 70, 1317–1341.
Wu, C.-C., Huang, Y.-H., Lien, G.-Y., 2012. Concentric eyewall formation in Typhoon Sinlaku (2008). Part I: Assimilation of T-PARC data based on the ensemble Kalman filter (EnKF). Monthly Weather Review 140, 506–527.